Molecular Phylogenetics and Evolution 94 (2016) 463–472

Contents lists available at ScienceDirect

Molecular Phylogenetics and Evolution

journal homepage: www.elsevier.com/locate/ympev

Phylogeographic surveys and apomictic genetic connectivity in the North Atlantic red seaweed *Mastocarpus stellatus* ☆

Jing-Jing Li [a,b,c], Zi-Min Hu [a,b,*], Ruo-Yu Liu [a,c], Jie Zhang [a,c], Shao-Lun Liu [d], De-Lin Duan [a,b,*]

[a] Key Laboratory of Experimental Marine Biology, Institute of Oceanology, Chinese Academy of Sciences, Qingdao 266071, China
[b] Qingdao National Laboratory for Marine Science and Technology, Qingdao 266071, China
[c] College of Earth Science, University of Chinese Academy of Sciences, Beijing 100049, China
[d] Department of Life Science, Tunghai University, Taichung 40704, Taiwan

ARTICLE INFO

Article history:
Received 4 December 2014
Revised 18 October 2015
Accepted 26 October 2015
Available online 31 October 2015

Keywords:
Apomictic propagation
Demographic history
Gene flow
Mastocarpus stellatus
Palaeoclimatic oscillation
Population genetic structure

ABSTRACT

The North Atlantic red alga *Mastocarpus stellatus* is characterized by two life histories (sexual-type and direct-type), which correspond to two geographically isolated breeding groups. These features enable *M. stellatus* to be an interesting model to investigate how environmental shift and apomictic propagation have influenced its population genetic structure, historical demography and distribution dynamic. To test these ideas, we obtained 456 specimens from 15 locations on both sides of the North Atlantic and sequenced portion of the nuclear internal transcribed spacer (ITS), mitochondrial *cox*2–3 region (COX) and plastid RuBisCo spacer (RLS). Median-joining networks and ML trees inferred from COX and RLS consistently revealed two gene lineages (mtDNA: C_N, C_S; cpDNA: R_N, R_S). The concatenated COX and RLS markers yielded three cytotypes: a northern C_N–R_N, a southern C_S–R_S and a mixed cytotype C_S–R_N, which enabled us to roughly separate samples into D (direct-type life-cycle) and S (sexual-type life-cycle) groups (northern C_N–R_N and mixed cytotype C_S–R_N = D; southern C_S–R_S = S). Pairwise F_{ST} analysis of the D group revealed a high level of genetic differentiation both along European coasts and across the Atlantic basin. Bayesian skyline plots (BSPs) and IMa analyses indicated that *M. stellatus* underwent slight demographic expansion at the late-Pleistocene, with the beginning of divergence between lineages dating to *c.* 0.189 Ma (95%HPD: 0.083–0.385 Ma). IMa analyses also revealed asymmetric genetic exchange among European populations and a predominant postglacial trans-Atlantic migration from Norway and Galway Bay to North America. Our study highlights the importance of phylogeographic approaches to discover the imprints of climate change, life histories and gene flow in driving population genetic connectivity and biogeographic distribution of intertidal seaweeds in the North Atlantic.

1. Introduction

Intertidal red seaweeds are usually characterized by complex haploid–diploid life cycles in which populations consist of dioecious haploid (gametophyte) and diploid (tetrasporophyte) individuals. Species of the genus *Mastocarpus* Kützing exhibit two types of life cycles which are inter-sterile (Guiry and West, 1983). In the first type, a heteromorphic life history is observed with dioecious foliose gametophytes and crustose sporophytes, hereafter referred as to the sexual-type. In the second type, a direct-type life history occurs in which carpospores on the female foliose plants germinate to form more female foliose plants without fertilization (Polanshek and West, 1977; Guiry and West, 1983; Zupan and West, 1988). These asexual gametophytes are more frequent at northern latitudes, and sexual gametophytes are more frequent at southern latitudes (Guiry and West, 1983; Zupan and West, 1988; Robba et al., 2006). Fierst et al. (2010) investigated mixed populations of *Mastocarpus papillatus* (C. Agardh) Kützing with both sexual and asexual variants at three sites along the central coast of California, and found that the variants were spatially separated within the intertidal zone. They found that sexual individuals were aggregated lower on the shore at two sites and only reproduced during part of a year, while asexual individuals occurred throughout the intertidal range at all sites and reproduced throughout the year. These features indicate that spatial and temporal partitioning may contribute to the long-term coexistence of sexual and asexual life histories in species

☆ This paper was edited by the Associate Editor Adrian Reyes-Prieto.

* Corresponding authors at: Key Laboratory of Experimental Marine Biology, Institute of Oceanology, Chinese Academy of Sciences, No. 7 Nanhai Road, Qingdao 266071, China. Fax: +86 532 82898556.
E-mail addresses: huzimin9712@163.com (Z.-M. Hu), dlduan@qdio.ac.cn (D.-L. Duan).

http://dx.doi.org/10.1016/j.ympev.2015.10.029
1055-7903/

of *Mastocarpus*, enabling them to be interesting models to investigate how climatic oscillations and apomictic propagation affected the distribution dynamic (e.g. range shifts, postglacial dispersal).

Recent phylogeographic studies have revealed two main scenarios for the marine biota with a trans-Atlantic distribution. In one, some marine taxa in the Northwestern Atlantic coast went extinct during glacial periods, and the area was recolonized from the Northeastern Atlantic during the Holocene (beginning about 11,500 years ago) (Wares and Cunningham, 2001; Teasdale and Klein, 2010). The other scenario is illustrated by organisms that survived in glacial refugia on both sides of the North Atlantic, for example, seaweeds (*Palmaria palmata*, Provan et al., 2005; Li et al., 2015; *Ascophyllum nodosum*, Olsen et al., 2010; *Chondrus crispus*, Hu et al., 2011a), sea urchins (Addison and Hart, 2005), and mussels (Riginos and Henzler, 2008). Phylogeographic studies have also showed that the direction of postglacial dispersal of European seaweed was mainly from the South to the North (Hoarau et al., 2007; Hu et al., 2011a; Provan and Maggs, 2012). However, the process of range shifts varied considerably among seaweeds, even though they exhibit similar geographic distribution. For example, *Fucus serratus* is an abundant fucoid dominating northern European shorelines. This species survived in the northern Brittany-Hurd Deep and the English Channel during the late Quaternary climate oscillations, and underwent an Irish refugium-sourced postglacial recolonization throughout Scandinavia via northern Scotland (Hoarau et al., 2007). In contrast, the red seaweed, *C. crispus*, which has a similar distribution range as *F. serratus* in the Northeast Atlantic, showed a postglacial stepping-stone recolonization from the English Channel refugium since the late Quaternary (Hu et al., 2011a; Provan and Maggs, 2012). Phylogeographic data retrieved from the red algae *Mastocarpus* may provide new insights into these contrasting evolutionary scenarios.

Mastocarpus stellatus (Stackhouse) Guiry is a common intertidal red alga on both sides of the North Atlantic, which shows two almost completely inter-sterile breeding groups in European coasts (Guiry and West, 1983; Fierst et al., 2010). In Northeastern Canada, only the "direct-type" life history was found (Chen et al., 1974; Guiry and West, 1983; Bird et al., 1994; Le Gall and Saunders, 2010). Previous studies illustrated that the direct-type plants tended to have higher rates of successful colonization in new areas than the sexual-type plants, as in some circumstance only one individual is needed to produce offspring and established a new population (Guiry and West, 1983). Considering the geographic separation of the sexual and asexual variants of *Mastocarpus*, the biogeographic histories of species of *Mastocarpus* may be quite different. The wide-range sampling of North Atlantic *M. stellatus* (40–70°N) provides an opportunity for us to detect how apomictic propagation impacted population genetic connectivity and phylogeographic structure of this species.

Morphologically, sexual plants of *M. stellatus* were redder in color, broader and fan-shaped, had more dichotomies and rounded apices; direct-type plants were more purplish-black in color, narrower and cuneate, had fewer dichotomies and pointed apices (Guiry and West, 1983). However, the features of sexual plants varied due to latitudinal differences, thus it becomes difficult to distinguish the two breeding groups based on morphological features (Zuccarello et al., 2005). Nevertheless, Zuccarello et al. (2005) found that the genetic differentiation between northern and southern European specimens strictly corresponded to two types of life histories in *M. stellatus*, indicating that the samples with different life cycles could be separated by organelle markers (mitochondrial *cox*2–3 spacer and plastid RuBisCo spacer). In addition, recent molecular studies also demonstrated high levels of nuclear genetic variance within *M. stellatus* (Lindstrom, 2008; Lindstrom et al., 2011), allowing us to use internal transcribed spacer (ITS) to survey nuclear DNA variability.

Based on intensive and wide-range sampling of *M. stellatus* along both sides of the North Atlantic (40–70°N), we aimed to examine if there were population-level genetic differentiation to support the north–south distribution pattern of the breeding groups. In particular, we tested two competitive hypotheses to explain the dominant apomictic reproduction of *M. stellatus* in Western Atlantic: (i) Northeastern Canadian populations went through a severe bottleneck and only "direct-type" plants survived the Quaternary ice ages; and (ii) present-day *M. stellatus* populations in Northeastern Canada resulted from postglacial migration from the Northeastern Atlantic of "direct-type" plants.

2. Materials and methods

2.1. Sampling and gene sequencing

Seaweed samples were collected from 15 locations on both sides of the North Atlantic (Fig. 1 and Table 1). At each location, 10–40 individuals were collected at *c.* 10 m intervals. Fronds were stored in silica gel. Total genomic DNA was extracted using the method developed by Hu et al. (2004). The fragment of the mitochondrial *cox*2–3 spacer (COX) was amplified using primers developed by Zuccarello et al. (1999a). Primers set ITS1 (5′-TCCGTAGGT GAACCTGCGG-3′) and JO6 (5′-ATATGCTTAAGTTCAGCGGGT-3′) described by Lindstrom and Hanic (2005), and primers set rbcF (5′ -TATACTTCTACAGACACAGCTGA-3′) and rbcR (5′-ATTTCACACAG GAAACAGCTATGACATGT-3′) described by Zuccarello et al. (1999b) were used to amplify ribosomal internal transcribed spacers (ITS) and plastid RuBisCo spacer (RLS), respectively. PCR, electrophoresis, product purification and sequencing were conducted according to previous protocols (Hu et al., 2007, 2011b). PCR products that failed direct sequencing due to multiple copies of ITS were cloned by TA-cloning system (Takara Biotechnology) following the manufacturer's instructions.

2.2. Genetic diversity and haplotype relatedness

Sequences were aligned in CLUSTAL X (Thompson et al., 1997) and manually edited in BioEdit 7.053 (Hall, 1999). The AMOVA and F_{ST} analyses were calculated using Arlequin 3.5 (Excoffier and Lischer, 2010). Modeltest 3.7 (Posada and Crandall, 1998) was used to identify the best substitution model for each locus under the Bayesian information criterion (BIC) (ITS: GTR + I: COX: GTR + G; RLS: HKY). Maximum likelihood (ML) and Bayesian inferences were performed to construct rooted genealogies for unique haplotypes using program PhyML 3.0 (Guindon et al., 2010) and MrBayes 3.2 (Ronquist et al., 2012), respectively. *Mastocarpus papillatus* [GenBank number: DQ872477 (ITS) and DQ884412 (RLS)] and *Chondrus crispus* [GenBank number: Z47547 (COX)] were chosen as out-groups. The ML tree was reconstructed using the selected model for each marker with 1000 bootstrap replicates. For BI analysis, Bayesian searches included four chains. Each chain was run for 2 million generations with a tree sampling frequency of every 100 generations. Then, 10% of the resulting trees were discarded as burin-in. The median-Joining network was examined for each locus with the program Network 4.51 (Bandelt et al., 1999).

2.3. Isolation-by-distance, divergence time and gene flow

Guiry and West (1983) found that most crosses between the two breeding groups (direct-type and sexual-type) were unsuccessful. Therefore, the two breeding groups should be regarded as different genetic entities for subsequent genetic analyses. Zuccarello et al. (2005) revealed that the two breeding groups had different RuBisCo and *cox*2–3 haplotypes, and that the "mixed"

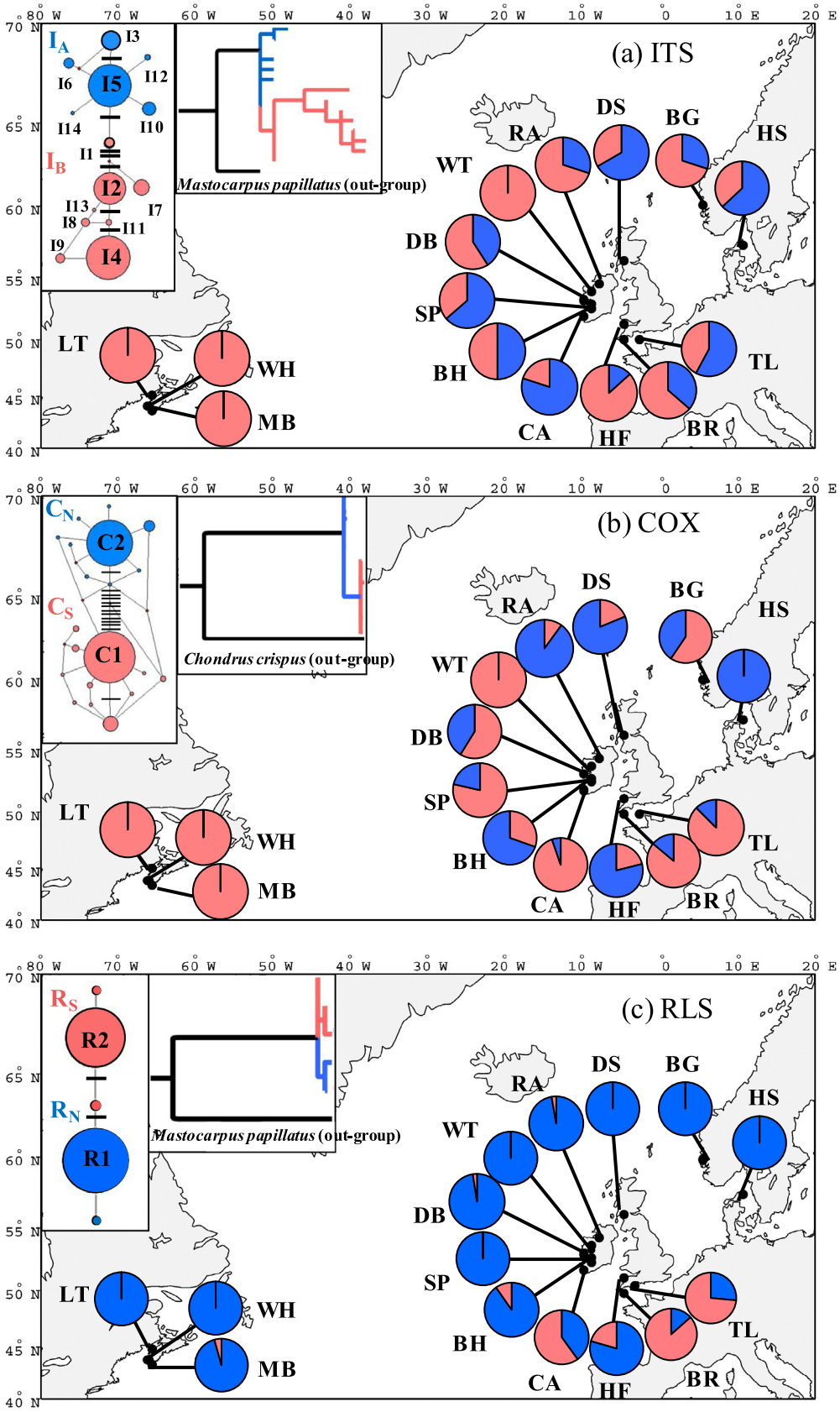

Fig. 1. Sampling localities and phylogenetic relationships among haplotypes of *Mastocarpus stellatus* inferred from ITS (a), COX (b) and RLS (c). The inset in upper left shows the median-joining network and ML trees. Each line between main haplotypes represents one mutation step. The size of each circle is proportional to haplotype frequency. The colored codes inside the network box indicate different groups (the northern type, blue; the southern type, pink). For each locality, the slice-size of pie-diagram is proportional to the frequency of lineages. Detailed locality information is shown in Table 1 (For interpretation of the references to colour in this figure legend, the reader is referred to the web version of this article.).

Table 1
Genetic diversity indices inferred from nrDNA ITS, mtDNA COX and cpDNA RLS data. N, Number of individuals; N_h, numbers of haplotypes; C_N–R_N, the northern cytotypes; C_S–R_S, the southern cytotypes; C_S–R_N, the mixed cytotypes; Haplotypes in bold belong to D group (direct-type life-cycle); others belong to the S group (sexual-type life-cycle).

Region/location	Code	Latitude	ITS		COX		RLS		Cytotypes		
			N	N_h	N	N_h	N	N_h	C_N–R_N	C_S–R_N	C_S–R_S
Bergen, Norway	BG	60.39°N/5.32°E	40	5	37	2	37	1	**15**	**22**	
Hirtshals, Denmark	HS	57.57°N/10.00°E	46	7	38	2	38	2	**37**		
Dunstaffnage Bay, Scotland	DS	56.46°N/−5.43°W	18	4	16	2	17	1	**13**	**3**	
Raghly, Sligo, Ireland	RA	54.33°N/−8.65°W	20	4	10	3	36	2	**9**	**1**	
Westport Quay, Ireland	WT	53.81°N/−9.55°W	7	1	20	2	20	1		**20**	
Dogs Bay, Ireland	DB	53.41°N/−9.9°W	22	3	17	7	41	2	**7**	**10**	
Spiddle, Ireland	SP	53.25°N/−9.31°W	11	2	14	8	34	1	**3**	**9**	
Black Head, Ireland	BH	53.18°N/−9.30°W	20	2	23	8	31	2	**16**	**4**	3
Carrigaholt, Ireland	CA	52.60°N/−9.71°W	20	3	19	5	30	2	**1**	**1**	17
Haverfordwest, England	HF	51.80°N/−5.00°W	15	2	38	3	39	2	**30**		8
Black Rock, England	BR	50.10°N/−5.34°W	33	4	36	3	37	3	**5**		31
Thurlestone, England	TL	50.27°N/3.86°W	37	5	32	4	34	2	**4**	**4**	24
Letete, Canada	LT	45.07°N/−66.90°W	9	1	9	1	9	1		**9**	
White Head Island, Canada	WH	44.65°N/−66.70°W	7	1	15	1	15	1		**15**	
St. Mary's Bay, Canada	MB	44.44°N/−66.20°W	24	2	23	1	23	2		**22**	1
All			329	14	347	20	441	5	**140**	**120**	84

haplotypes (northern plastid haplotype with southern mitochondrial haplotype) were found only in plants with direct-type life-cycle. We then roughly assembled the samples with northern and mixed cytotypes as one group (D group, samples with direct-type life-cycle) and the southern cytotypes as the other group (S groups, samples with sexual-type life-cycle).

Because the samples with sexual-type plants were restricted to the English Channel (Table 1), we only used the data of D group to test the isolation-by-distance (IBD) model (Bohonak, 2002). IBD was carried out to test the hypothesis of a stepping-stone model of gene flow between European *M. stellatus* populations. A Mantel test was performed using Arlequin with one thousand permutations to assess the relationship between genetic distances, measured as $F_{ST}/(1-F_{ST})$, and geographical distances (minimum coastline distance) between populations.

An isolation-with-migration model, as implemented in IMa 2 (Nielsen and Wakeley, 2001; Hey and Nielsen, 2007; Hey, 2010), was used to estimate the divergence time (t), migration rates (m) and population sizes (Θ), based on the organelle markers (running as independent loci). Due to insufficient information on evolutionary relationships among *M. stellatus* populations, we performed pairwise comparisons between groups. For each run, we used a series of initial IMa runs in 'MCMC mode' to determine the most efficient search parameters that maximized mixing: first, we set broad prior probabilities for population parameters (t, Θ and m), and subsequently reset the upper bounds according to the former results to get more intensive posteriors. We ran five replicates with different random seeds in order to check the consistency among runs. A total of 100,000 genealogies were sampled to estimate joint posterior probability distributions of migration parameters. To convert the divergence time to absolute time scale, we used estimates of mutation rates (μ) for other relevant red seaweeds, with a 4.7×10^{-9} substitutions/site/year (s/s/y) for ITS (Hu et al., 2010), 5.5×10^{-9} s/s/y for COX (Zuccarello and West, 2002) and 1.2×10^{-9} s/s/y for RLS (Kamiya et al., 2004), although interspecific clock rates may be slower than pedigree clock rates (Howell et al., 2003; Ho et al., 2005; Grant, 2015).

2.4. Demographic history

Current (θ_π) and historical (θ_W) genetic diversities were estimated with DnaSP v5.0 (Librado and Rozas, 2009). Comparing these two estimates could provide insights into population dynamics: recent bottlenecks (if $\theta_\pi < \theta_W$) or recent population growth (if $\theta_\pi > \theta_W$) (Templeton, 1993; Pearse and Crandall, 2004). The departure from population demographic equilibrium was assessed using Fu's *Fs* (Fu, 1997) and Tajima's *D* (Tajima, 1989) statistics in Arlequin with 1000 coalescent simulations. The two statistics identify excesses of recent low-frequency mutations resulting from a population expansion, or natural selection (Pearse and Crandall, 2004; Templeton, 1993). In addition, we also investigated population demographic growth through a mismatch distribution using Arlequin. A multimodal distribution generally indicates that the population is at demographic equilibrium, while a unimodal distribution is the signature of recent demographic or range expansion or a selective sweep (Rogers and Harpending, 1992; Ray et al., 2003; Excoffier, 2004).

We also used beast v1.7.4 (Drummond and Rambaut, 2007; Heled and Drummond, 2008) to generate Bayesian skyline plots (BSP) to depict demographic history. The MCMC parameters were set as follows: 8×10^8 iterations, sampling every 4000 iterations. The analyses were carried out three times using different random seeds, and the results were pooled using LogCombiner to increase the effective sample sizes (ESS) of each parameter (>200). Convergence was assessed by TRACER v1.5 (Drummond et al., 2005) with burn-in of 10% chains.

3. Results

3.1. Haplotype network, divergence time and linkage disequilibria

The entire ribosomal ITS1-5.8S-ITS2 region was successfully amplified and the length of 5.8S rDNA coding region consisted of 159 bp. Due to different mutation rates between coding and non-coding regions, we only used ITS1 and ITS2 regions for subsequent genetic analyses. Aligned ITS1 and ITS2 sequences produced 541 bp with 14 variable sites, yielding 14 haplotypes in 329 individuals of *M. stellatus* (GenBank accession numbers KP121917–KP121930). A major part of the variation in the sequences was the indels (8/14). Populations from Canada (MB, WH, LT) harbored two haplotypes, one of which was endemic (I13; Table A.1 in Appendix A). The median-joining network, ML and BI cladograms consistently separated the 14 haplotypes into two major lineages. Except for three samples from Canada (MB, WH, LT), which are characterized with high genetic homogeneity, most European *M. stellatus* samples exhibited a mixture of two lineages in each location (Fig. 1a and Table 2). In contrast with organellar markers (see below), the two lineages detected by ITS (I_A and I_B) did no coincide with the assignation of the two breeding groups.

Table 2
The distribution of the combined ITS-COX-RLS types in *Mastocarpus stellatus* populations. Haplotypes in bold belong to D group (direct-type life-cycle); others belong to the S group (sexual-type life-cycle).

Region/location	Code	ITS-COX-RLS types					
		I_A–C_N–R_N	I_A–C_S–R_N	I_A–C_S–R_S	I_B–C_N–R_N	I_B–C_S–R_N	I_B–C_S–R_S
Bergen, Norway	BG	**9**	**4**		**5**	**18**	
Hirtshals, Denmark	HS	**23**			**14**		
Dunstaffnage Bay, Scotland	DS	**10**	**2**		**3**	**1**	
Raghly, Sligo, Ireland	RA	**3**			**6**		
Westport Quay, Ireland	WT					**7**	
Dogs Bay, Ireland	DB	**7**	**2**		**2**	**6**	
Spiddle, Ireland	SP	**3**	**4**			**4**	
Black Head, Ireland	BH	**10**			**8**		
Carrigaholt, Ireland	CA		**1**	14			3
Haverfordwest, England	HF			2	**12**		
Black Rock, England	BR			11	**2**		17
Thurlestone, England	TL		**2**	18	**4**	**2**	5
Letete, Canada	LT					**9**	
White Head Island, Canada	WH					**7**	
St. Mary's Bay, Canada	MB					**22**	1
All		**65**	**15**	45	**56**	**76**	26

The 364 bp of mtDNA *cox*2–3 fragment yielded 18 variable sites from 347 individuals of *M. stellatus* and resulted in 20 haplotypes (GenBank accession numbers KP121897–KP121916). Of these haplotypes, 12 (60%) were unique and two (C1 and C2) were present in 87% of the sampling locations (Table A.2 and Fig. 1b). Only one haplotype (C1) was detected in North America but was shared with most European populations (Table A.2). Although the network recovered two separate genetic lineages (differed by 11 bp, Table A.3), which corresponded to the two breeding groups, they did not show a clear north–south distribution pattern (Fig. 1b). The core haplotypes detected in the northern (C2) and southern (C1) lineage (Fig. 1b) exactly corresponded to the northern ($C1^Z$) and southern haplotype ($C2^Z$) inferred from the two breeding groups of *M. stellatus* by Zuccarello et al. (2005) (Table A.3), except for 2-bp indel in $C1^Z$ (Table A.3).

For cpDNA RuBisCo spacer (RLS), 441 sequences of 290-bp length contained four variable sites and generated five haplotypes (GenBank accession numbers KP121931–KP121935). Haplotype diversity varied among populations, but generally showed a trend of decreasing diversity from southern to northern Europe (Table A.4 and Fig. 1c). The haplotype tree and network analyses identified two genetically split lineages (differed by 1 bp, Table A.5) which showed a pronounced north–south distribution pattern (Fig. 1c). Interestingly, one lineage had a wide-distribution across North Atlantic, while the other was restricted to the British Isles and southwest Ireland (Fig. 1c). The core haplotypes detected in the northern (R1) and southern (R2) lineage (Fig. 1c) exactly corresponded to the northern ($R1^Z$) and southern haplotype ($R2^Z$) inferred from the two breeding group samples of *M. stellatus* by Zuccarello et al. (2005) (Table A.5). Since the cladograms inferred from ML and BI showed similar haplotype relationships for each gene marker, we presented only the ML trees in this paper (Fig. 1).

The haplotypes inferred from cytoplasmic markers were divided into northern (C_N, R_N) and southern (C_S, R_S) haplotypes based on networks (Fig. 1). Theoretically, no "mixed" types should be found if there were strict linkages between northern and southern cytotypes (C_N–R_N, C_S–R_S). However, we identified many individuals with mixed cytotypes (Table 1). The three main cytotypes were: C_N–R_N, which were found only in European populations with higher frequency in Northern areas (Table 1); C_S–R_S, which were found only in southern areas (English Channel and southern Galway Bay); the "mixed" cytotype C_S–R_N, which was mainly found in northern Europe and northeastern Canada (Table 1). Another mixed cytotype C_N–R_S was only present in one sample from BR.

Overall, the organelle markers consistently revealed two genetic lineages in *M. stellatus* populations. The concatenated data sets suggested that the split time between them dated back to *c.* 0.189 Ma (95%HPD: 0.083–0.385 Ma), corresponding to the Saale glacial period (0.130–0.191 Ma) (Fig. 2).

3.2. Population divergence and Gene flow

Pairwise F_{ST} values were calculated using samples from the D group (Table A.6). F_{ST} based on the ITS and COX sequences revealed medium-to-high levels of genetic differentiation among European populations, even between geographically nearby populations, e.g. WT-RA (ITS: $F_{ST} = 0.402$; COX: $F_{ST} = 0.912$) and HF-TL (ITS: $F_{ST} = 0.680$; COX: $F_{ST} = 0.664$) (Table A.6). Significant genetic divergence was also detected between North American and European populations, except for Ireland (WT), which showed closer genetic affinity with North American than other European populations (Table A.6). F_{ST} values between North American population pairs were generally low and non-significant (Table A.6). In addition, all F_{ST} values based on RLS marker were smaller than 0.001 (data not shown). Separate AMOVA analyses based on RLS among S and D group haplotypes consistently indicated that most of the genetic variance was within populations (Table 3), with the largest divergence between the D and S groups ($\Phi_{CT} = 0.982$, $p < 0.0001$; Table 3). The deep split between the two groups was also apparent for COX ($\Phi_{CT} = 0.341$, $p = 0.03$), and accounted for 34.06% of the variance (Table 3). As a comparison, separate AMOVA analyses based on COX showed significant divergence among D-group populations ($\Phi_{ST} = 0.630$, $p < 0.0001$; Table 3), and significant variance within populations for S groups (Table 3). For ITS, a significant pattern of variance was detected only within populations (Table 3).

The test for IBD among European populations was non-significant (Mantel's correction coefficient's $p > 0.05$) (Fig. A.1 in Appendix A). In order to detect genetic exchange between regions, we calculated gene flow between six regions using the organelle markers: Norway (NOR), Denmark (DEN), Scotland (SCO), Galway Bay (GAL), English Channel (ENC) and North America (NA). Trans-Atlantic gene flow (*Nm*) was detected mainly from Europe to North America (Fig. 3). The main donor sites were Norway and the Galway Bay (NOR → NA: $Nm = 0.852$, 95% HPD: 0.078–1.831; GAL → NA: $Nm = 1.076$, 95% HPD: 0.701–2.269), and the migration rate was four times larger than that from Scotland to North America ($Nm = 0.211$, 95% HPD: 0.031–0.960). The posterior probability distribution for gene flow in the opposite direction lacked a single

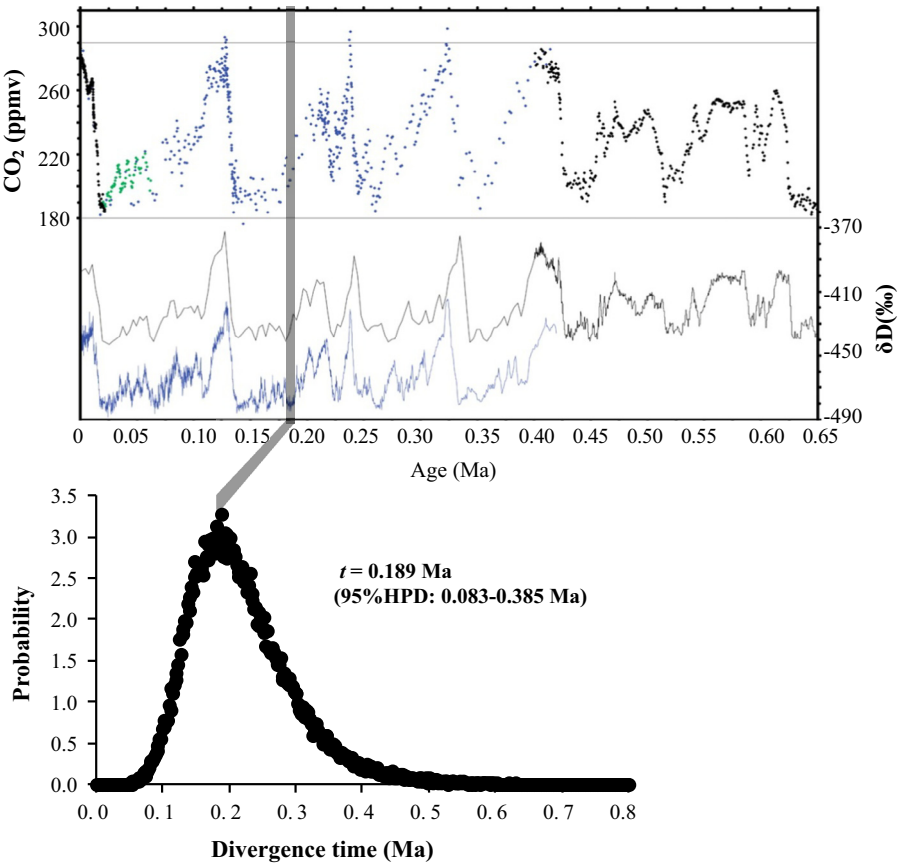

Fig. 2. Posterior probability distributions for divergence time of organelle lineages, estimated using IMa 2. The composite CO_2 record (the graph above) was adapted from Siegenthaler et al. (2005).

Table 3
Hierarchical analysis of molecular variance (AMOVA) revealed by mtDNA *cox*2–3 (COX), plastid RuBisCo spacer (RLS) and ITS1 + ITS2 (ITS) from North Atlantic *Mastocarpus stellatus*, respectively. S group: samples with sexual-type life-cycle; D group: samples with direct-type life-cycle.

Structure	Among regions			Among populations within regions			Within populations		
	d.f.	%var	Φ_{CT}	d.f.	%var		d.f.	%var	Φ_{ST}
COX									
S group	_	_	_	3	20.22	$F_{ST} = 0.202^{**}$	76	79.78	_
D group	_	_	_	13	62.98	$F_{ST} = 0.630^{***}$	243	37.02	_
S–D group	1	34.06	0.341n.s.	16	42.43	$\Phi_{SC} = 0.644^{***}$	319	23.51	0.765^{***}
RLS									
S group	_	_	_	3	−4.11	$F_{ST} = -0.041$n.s.	76	104.11	_
D group	_	_	_	12	−2.24	$F_{ST} = -0.022$n.s.	239	102.24	_
S–D group	1	98.25	0.982^{***}	15	−0.05	$\Phi_{SC} = -0.031$n.s	315	1.81	0.982^{***}
ITS									
S group	_	_	_	2	14.86	$F_{ST} = 0.149^{*}$	67	85.14	_
D group	_	_	_	12	39.02	$F_{ST} = 0.390^{***}$	198	60.98	_
S–D group	1	2.27	0.023n.s.	14	32.09	$\Phi_{SC} = 0.328^{***}$	265	65.64	0.344^{***}

n.s., not significant; %var, percentage of variance; Φ_{CT}, genetic variance among regions; Φ_{SC}, genetic variance among populations within regions; Φ_{ST}, genetic variance within populations; F_{ST}, genetic variance among populations.

* $p < 0.01$.
** $p < 0.001$.
*** $p < 0.0001$.

clear peak, indicating no genetic exchange (data not shown). There was asymmetrical genetic exchange between populations in northern Europe (NOR, SCO and DEN) (Fig. 3). The populations in Norway and Scotland showed high levels of outward genetic migration to Denmark (NOR→DEN: $Nm = 0.643$, 95% HPD: 0.066–3.339; SCO → DEN: $Nm = 0.454$, 95% HPD: 0.000–1.349). In contrast, there was restricted genetic exchange between the three populations in the British Isles (SCO, GAL, ENC), with *Nm* varying from 0.113 to 0.313. The population from the Galway Bay had the highest effective population size compared with other populations ($\Theta = 0.88$, 95% HPD = 0.08–6.99, Fig. 3), while populations in North America and the English Channel had the smallest Θ values (NA: $\Theta = 0.02$, 95% HPD = 0.00–0.32; ENC: $\Theta = 0.02$, 95% HPD = 0.00–0.10).

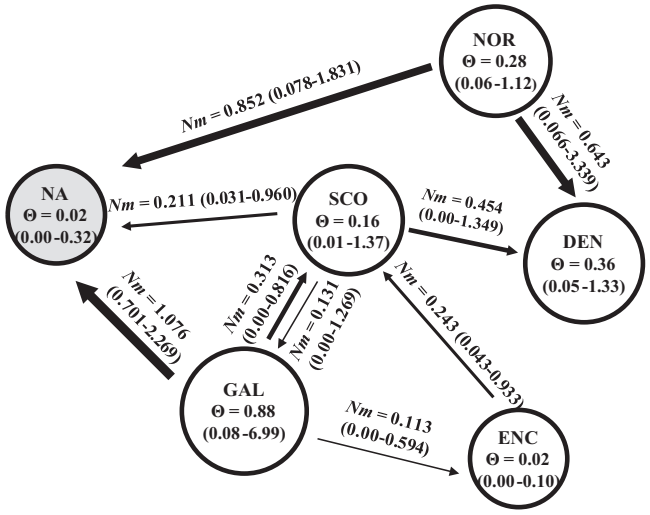

Fig. 3. Historical effective population size (Θ) and gene flow (Nm) for D groups (samples with direct-type life history) between six regions (95% confidence intervals in parentheses) inferred from IMa 2. For clarity of presentation Nm values less than 1 are not shown. NOR: Norway; DEN: Denmark; SCO: Scotland; GAL: Galway Bay; ENC: English Channel; NA: North America (North American populations are shown in light gray).

3.3. Demographic history

As only a few haplotypes and variable nucleotides were detected in RLS, the demographic history of *M. stellatus* was estimated based on COX and ITS data sets. BSP analysis inferred for different clades consistently revealed a slight population expansion *c.* 0.25–0.35 Ma (Fig. A.2). The neutral Tajima's *D* and Fu's *Fs* tests exhibited the signs of sudden population expansion (Table 4). However, the mismatch distribution of the two data sets showed no signs of recent demographic or range expansion (Fig. A.3). The comparisons of current (θ_π) and historical (θ_W) genetic diversities indicated a recent population size expansion as well because θ_π was substantially larger than θ_W (Table 4).

4. Discussion

4.1. Hybridization and lineage distribution

The multiple life-history types in seaweeds are an important biological mechanism to adapt to variable intertidal environments (Ludington et al., 2004). Guiry and West (1983) first reported two types of life histories in *M. stellatus*, corresponding to a north–south distribution pattern in Europe. Recent molecular data detected genetic differentiation between northern and southern European specimens, exactly corresponding to two types of life histories in *M. stellatus* (Zuccarello et al., 2005). In this paper, RLS data provided population-level phylogeographic evidence on the north–south distribution of two lineages despite COX analysis showed that 'southern' haplotypes were also widely distributed in North Europe. One possible explanation for the appearance of the 'mixed' cytoplasmic genome is the hybridization between asexual-type plants in the North and direct-type plants from the South mediated by human activities (Johnson et al., 2012). As a matter of fact, the hybridization of the two breeding groups has been also reported under laboratory culture (Guiry and West, 1983). Interestingly, we found only one type of mixed cytotypes (C_S–R_N). Although organelle genomes are preferentially transmitted maternally for oogamous species (Zuccarello et al., 1999a; Choi et al., 2008; Destombe et al., 2010), the paternal inheritance of mtDNA have also been reported in seaweed, e.g. *Fucus serratus* × *F. evanescens* (Hoarau et al., 2009). The paternal inheritance of mtDNA might also occur in *M. stellatus* during the hybridization of the two breeding groups, and the mixed cytotypes (C_S–R_N) were fixed in the D group through genetic introgression of the southern haplotype (C_S).

Table 4
Neutral tests and demographic estimates for *Mastocarpus stellatus* based on ITS and COX lineages. Estimates of current (θ_π) and historical (θ_W) genetic diversities. Codes are identical to Fig. 1.

Clade	Tajima's *D*	Fu's *Fs*	θ_π	θ_W
C_N	−1.883*	−11.557***	0.00056	0.00351
C_S	−1.508*	−11.115***	0.00094	0.00327
I_A	−1.023 ns	−0.698 ns	0.00128	0.00278
I_B	0.882 ns	3.612 ns	0.00317	0.00257

ns, not significant.
* $p < 0.05$.
*** $p < 0.0001$.

Mastocarpus stellatus in Nova Scotia, Canada has been reported as wholly apomictic (Chen et al., 1974). In particular, the three Canadian *M. stellatus* populations were overwhelmingly dominated by mixed cytotypes (belonging to D group) (Table 1). Such distinctive distribution may have resulted from the recolonization from European "direct-type" plants (see below for details). In addition, the detected geographic distribution of individuals with direct-type life-cycle is consistent with Baker's Law that the colonization by self-compatible organisms is more likely to be successful than the colonization by self-incompatible organisms (Baker, 1967). In reality, direct-type plants of *M. stellatus* are similar to self-compatible organisms and require only one fertile female for successful colonization, leading to the dominant distribution in the coasts of Nova Scotia, Canada.

4.2. Population genetic differentiation and geographic expansion in Europe

Marine macroalgae characterized with limited dispersal potential tend to show a pattern of isolation by distance (IBD), where populations exhibiting geographical proximity are more genetically similar than those separated by longer distances. For example, Krueger-Hadfield et al. (2011) observed a weak but significant IBD pattern in *Chondrus crsipus* at a fine geographical scale (from a few hundred meters to approximately 200 km). Similar profiles have also been identified in other red seaweeds, including *Ahnfeltiopsis pusilla* (Couceiro et al., 2011), *Gelidium canariense* (Bouza et al., 2006) and *Mazzaella laminarioides* (Faugeron et al., 2001). However, populations in non-equilibrium conditions will lose IBD when genetic drift is greater than gene flow (Wares, 2002). Recent studies demonstrated that IBD signal of population structure begins to fade at distance >100 km for most intertidal seaweeds (Fraser et al., 2010; Olsen et al., 2010; Neiva et al., 2012). In this study, we did not find a connection between geographic distance and genetic variance in *M. stellatus* at large geographical scales (Fig. A.1). A previous study indicated that *M. stellatus* plants with a sexual life history in New England occurred only in the low intertidal zone and asexual individuals occurred in the higher intertidal zone (Dudgeon et al., 1995). Interestingly, this phenomenon has also been reported in the congeneric species *M. papillatus* (Fierst et al., 2010). These observations indicate that the high level of genetic differentiation between populations within geographic proximity may be mainly driven by the topography of shoreline along Europe that created microhabitat patches, and thus influenced the dispersal and colonization of sexual and asexual spores in the intertidal zone (Brawley and Johnson, 1991;

Johnson, 1994; McNair et al., 1997; Johnson and Brawley, 1998; Dudgeon et al., 2001; Dudgeon and Petraitis, 2005).

Phylogeographic studies illustrated two main postglacial expansion routes along European coasts for intertidal seaweeds: one expansion originated from the Galway Bay via northern Scotland to Scandinavia; the other expansion started from the northern Brittany-Hurd Deep refugium, and spread westward and northward into the eastern Ireland, western Scotland, eastern England and the main European coasts (*F. serratus*, Hoarau et al., 2007; *P. palmata*, Provan et al., 2005; *C. crispus*, Provan and Maggs, 2012; *Pelvetia canaliculata*, Neiva et al., 2014). The overall feature is that all these seaweeds expanded from southern glacial refugia, leading to a south-to-north migration. In contrast, in this study the genetic exchange of D group between regions was mainly detected among North Europe, and the populations in Norway (NOR) and Galway Bay (GAL) were major contributed migrants for postglacial recolonization (Fig. 3). This implies that Bergen or adjoining islands may have served as a glacial refugium for *M. stellatus* populations. In fact, numerous molecular surveys on seaweeds supported the existence of such a potential refugium in Norway and the Faroe Islands (Maggs et al., 2008; Olsen et al., 2010; Coyer et al., 2011; Hu et al., 2013). Physiologically, more tolerance of environmental stress, such as freezing and desiccation, may have allowed *M. stellatus* to survive in the northern Atlantic glacial refugium compared with the co-distributed red alga *C. crispus* (Davison et al., 1989; Dudgeon et al., 1989, 1990; Collen and Davison, 1999; Lohrmann et al., 2004).

4.3. Demographic history and trans-Atlantic migration

Our molecular data sets consistently revealed that *M. stellatus* experienced a sudden population expansion during the mid-Pleistocene (*c.* 0.25–0.35 Ma). Such a timescale is comparable to that estimated for the red alga *C. crispus* (*c.* 0.350–0.415 Ma) (Hu et al., 2010), which has an analogous geographic distribution with *M. stellatus*. This expansion time is much earlier than the one estimated in North Atlantic brown seaweeds. For example, multi-data sets indicate that both *F. vesiculosus* and *F. serratus* experienced a pre-LGM interglacial demographic expansion (Eerm, 0.068–0.128 Ma) (Hoarau et al., 2007; Coyer et al., 2011). The sequential time expansion may imply that the demographic history of red and brown seaweeds in the North Atlantic was predominantly shaped by Mid-to-Late Pleistocene (*c.* 0.84–0.13 Ma) glacial episodes.

The haplotypes detected in North America are not only shared with European coasts, but also exhibit a wide distribution range (Fig. 1). Besides, we detected that North American populations were dominated by mixed cytotypes. Similar results were also obtained by Le Gall and Saunders (2010), who also found only one genetic group in eastern Canada. We infer that historically North American *M. stellatus* populations had been totally eradicated by rising sea level during the Quaternary ice age, and the current observed populations in St. Mary's Bay resulted from the postglacial trans-Atlantic migration from European coasts. Such an east-to-west dispersal has been increasingly discovered in North Atlantic intertidal organisms. For example, recent phylogeographic studies confirmed a similar pattern in brown seaweeds *F. vesiculosus* (Coyer et al., 2011) and *A. nodosum* (Olsen et al., 2010), and the gastropods *Nucella lapillus* and *Littorina obtusata* (Wares and Cunningham, 2001). Interestingly, the detected postglacial migration pathways in *M. stellatus* highly resemble another North Atlantic red seaweed, *Porphyra umbilicalis*: The genetic data supports bi-directional dispersal of Norway populations southward to other parts of Europe and westward as the donor populations for North America (Teasdale and Klein, 2010). The haplotype distribution and coalescent analyses also indicated Norway as a likely donor for postglacial migration to North America in *M. stellatus*. This migration route is consistent with the results observed in *C. crispus* (Provan and Maggs, 2012). The extremely lower genetic differentiation (Table A.6) between North American *M. stellatus* populations suggests that the trans-Atlantic migration must just have happened during the past few hundred years and was probably mediated by anthropogenic activities. Such a dispersal mechanism is similar to the introduction of *F. serratus* from western Ireland to Canadian Maritime Provinces using rocks as ballast in shipping (Brawley et al., 2009), an efficient way to increase the dispersal distance for macroalgae (Johnson et al., 2012).

5. Conclusions

Population genetic differentiation and geographic distribution of *Mastocarpus stellatus* is an interactive process of palaeoclimatic oscillation, biological features, genetic exchange and shoreline topography. Multilocus data sets can help to identify some unique genetic insights into adaptive distribution and evolution of seaweed's life history in North Atlantic. The detected north-to-south distribution of two life-history types in *M. stellatus* along European coasts may provide some aspects to decipher the potential modes, mechanisms and dynamic processes of organellar genomic recombinations.

Acknowledgments

We are grateful to K. Sjøtun (Department of Biology, University of Bergen) and A. T. Critchley (Canada Acadian Seaplants Limited) for helping collect some seaweed specimens. Special thanks go to J. Lopez-Bautista (the University of Alabama at Tuscaloosa) and Y. S. Xiao for their critical proofs and comments on the manuscript. We are grateful to editors and two anonymous referees for providing valuable feedback that improved the manuscript. Funding was supplied by the Natural Science Foundation of China (31000103 and 31370264) Granted to Z.M. Hu.

Appendix A. Supplementary material

Supplementary data associated with this article can be found, in the online version, at http://dx.doi.org/10.1016/j.ympev.2015.10.029.

References

Addison, J.A., Hart, M.W., 2005. Colonization, dispersal, and hybridization influence phylogeography of North Atlantic sea urchins (*Strongylocentrotus droebachiensis*). Evolution 59, 532–543.
Baker, H.G., 1967. Support for Baker's law as a rule. Evolution 21, 853–856.
Bandelt, H.-J., Forster, P., Röhl, A., 1999. Median-joining networks for inferring intraspecific phylogenies. Mol. Biol. Evol. 16, 37–48.
Bird, C.J., Sosa, P.A., Mackay, R.M., 1994. Molecular evidence confirms the relationship of *Petrocelis* in the western Atlantic to *Mastocarpus stellatus* (Rhodophyta, Petrocelidaceae). Phycologia 33, 134–137.
Bohonak, A.J., 2002. IBD (isolation by distance): a program for analyses of isolation by distance. J. Hered. 93, 153–154.
Bouza, N., Caujapé-Castells, J., González-Pérez, M.A., Sosa, P.A., 2006. Genetic structure of natural populations in the red algae *Gelidium canariense* (Gelidiales, Rhodophyta) investigated by random amplified polymorphic DNA (RAPD) markers. J. Phycol. 42, 304–311.
Brawley, S.H., Coyer, J.A., Blakeslee, A.M.H., Hoarau, G., Johnson, L.E., Byers, J.E., Stam, W.T., Olsen, J.L., 2009. Historical invasions of the intertidal zone of Atlantic North America associated with distinctive patterns of trade and emigration. Proc. Natl. Acad. Sci. USA 106, 8239–8244.
Brawley, S.H., Johnson, L.E., 1991. Survival of fucoid embryos in the intertidal zone depends upon developmental stage and microhabitat. J. Phycol. 27, 179–186.
Chen, L.C.-M., Edelstein, T., Mclachlan, J., 1974. The life history of *Gigartina stellata* (Stackh.) Batt. (Rhodophyceae, Gigartinales) in culture. Phycologia 13, 287–294.
Choi, S.J., Park, E.J., Endo, H., Kitade, Y., Saga, N., 2008. Inheritance pattern of chloroplast and mitochondrial genomes in artificial hybrids of *Porphyra yezoensis* (Rhodophyta). Fish. Sci. 74, 822–829.

Collen, J., Davison, I.R., 1999. Stress tolerance and reactive oxygen metabolism in the intertidal red seaweeds *Mastocarpus stellatus* and *Chondrus crispus*. Plant Cell Environ. 22, 1143–1151.

Couceiro, L., Maneiro, I., Ruiz, J.M., Barreiro, R., 2011. Multiscale genetic structure of an endangered seaweed *Ahnfeltiopsis pusilla* (Rhodophyta): implications for its conservation. J. Phycol. 47, 259–268.

Coyer, J.A., Hoarau, G., Costa, J.F., Hogerdijk, B., Serrão, E.A., Billard, E., Valero, M., Pearson, G.A., Olsen, J.L., 2011. Evolution and diversification within the intertidal brown macroalgae *Fucus spiralis/F. vesiculosus* species complex in the North Atlantic. Mol. Phylogenet. Evol. 58, 283–296.

Davison, I.R., Dudgeon, S.R., Ruan, H.M., 1989. Effect of freezing on seaweed photosynthesis. Mar. Ecol. Prog. Ser. 58, 123–131.

Destombe, C., Valero, M., Guillemin, M.L., 2010. Delineation of two sibling red algal species, *Gracilaria gracilis* and *Gracilaria dura* (Gracilariales, Rhodophyta), using multiple DNA markers: resurrection of the species *G. dura* previously described in the northern Atlantic 200 years ago. J. Phycol. 46, 720–727.

Drummond, A.J., Rambaut, A., 2007. BEAST: Bayesian evolutionary analysis by sampling trees. BMC Evol. Biol. 7, 214.

Drummond, A.J., Rambaut, A., Shapiro, B., Pybus, O.G., 2005. Bayesian coalescent inference of past population dynamics from molecular sequences. Mol. Biol. Evol. 22, 1185–1192.

Dudgeon, S., Kübler, J.E., Wright, W.A., Vadas, R.L., Petraitis, P.S., 2001. Natural variability in zygote dispersal of *Ascophyllum nodosum* at small spatial scales. Funct. Ecol. 15, 595–604.

Dudgeon, S., Petraitis, P.S., 2005. First year demography of the foundation species, *Ascophyllum nodosum*, and its community implications. Oikos 109, 405–415.

Dudgeon, S.R., Davison, I.R., Vadas, R.L., 1989. Effect of freezing on photosynthesis of intertidal macroalgae: relative tolerance of *Chondrus crispus* and *Mastocarpus stellatus* (Rhodophyta). Mar. Biol. 101, 107–114.

Dudgeon, S.R., Kübler, J.E., Vadas, R.L., Davison, I.R., 1995. Physiological responses to environmental variation in intertidal red algae: dose thallus morphology matter. Mar. Ecol. Prog. Ser. 117, 193–206.

Dudgeon, T.J., Cooke, R.M., Baron, M., Campbell, I.D., Edwards, R.M., Fallon, A., 1990. Structure-function analysis of epidermal growth factor: site directed mutagenesis and nuclear magnetic resonance. FEBS Lett. 261, 392–396.

Excoffier, L., 2004. Patterns of DNA sequence diversity and genetic structure after a range expansion: lessons from the infinite-island model. Mol. Ecol. 13, 853–864.

Excoffier, L., Lischer, H.E.L., 2010. Arlequin suite ver 3.5: a new series of programs to perform population genetics analyses under Linux and Windows. Mol. Ecol. Resour. 10, 564–567.

Faugeron, S., Valero, M., Destombe, C., Martínez, E.A., Correa, J.A., 2001. Hierarchical spatial structure and discriminant analysis of genetic diversity in the red alga *Mazzaella laminarioides* (Gigartinales, Rhodophyta). J. Phycol. 37, 705–716.

Fierst, J.L., Kubler, J.E., Dudgeon, S.R., 2010. Spatial distribution and reproductive phenology of sexual and asexual *Mastocarpus papillatus* (Rhodophyta). Phycologia 49, 274–282.

Fraser, C.I., Thiel, M., Spencer, H.G., Waters, J.M., 2010. Contemporary habitat discontinuity and historic glacial ice drive genetic divergence in Chilean kelp. BMC Evol. Biol. 10, 203.

Fu, Y.-X., 1997. Statistical tests of neutrality of mutations against population growth, hitchhiking and background selection. Genetics 147, 915–925.

Guindon, S., Dufayard, J.F., Lefort, V., Anisimova, M., Hordijk, W., Gascuel, O., 2010. New algorithms and methods to estimate maximum-likelihood phylogenies: assessing the performance of PhyML 3.0. Syst. Biol. 59, 307–321.

Guiry, M.D., West, J.A., 1983. Life history and hybridization studies on *Gigartina stellata* and *Petrocelis cruenta* (Rhodophyta) in the North Atlantic. J. Phycol. 19, 474–494.

Grant, W.S., 2015. Problems and cautions with sequence mismatch analysis and bayesian skyline plots to infer historical demography. J. Hered. 106, 333–346.

Hall, T.A., 1999. BioEdit: a user-friendly biological sequence alignment editor and analysis program for Window 95/98/NT. Nucl. Acids Symp. Ser. 41, 95–98.

Heled, J., Drummond, A.J., 2008. Bayesian inference of population size history from multiple loci. BMC Evol. Biol. 8, 289.

Hey, J., 2010. Isolation with migration models for more than two populations. Mol. Biol. Evol. 27, 905–920.

Hey, J., Nielsen, R., 2007. Integration within the Felsenstein equation for improved Markov chain Monte Carlo methods in population genetics. Proc. Natl. Acad. Sci. USA 104, 2785–2790.

Ho, S.Y.W., Phillips, M.J., Cooper, A., Drummond, A.J., 2005. Time dependency of molecular rate estimates and systematic overestimation of recent divergence times. Mol. Biol. Evol. 22, 1561–1568.

Hoarau, G., Coyer, J.A., Veldsink, J.H., Stam, W.T., Olsen, J.L., 2007. Glacial refugia and recolonization pathways in the brown seaweed *Fucus serratus*. Mol. Ecol. 16, 3606–3616.

Hoarau, G., Coyer, J.A., Olsen, J.L., 2009. Paternal leakage of mitochondrial DNA in a *Fucus* (Phaeophyceae) hybrid zone. J. Phycol. 45, 621–624.

Howell, N., Smejkal, C.B., Mackey, D.A., Chinnery, P.F., Turnbull, D.M., Herrnstadt, C., 2003. The pedigree rate of sequence divergence in the human mitochondrial genome: there is a difference between phylogenetic and pedigree rates. Am. J. Hum. Genet. 72, 659–670.

Hu, Z.M., Critchley, A.T., Gao, T.X., Zeng, X.Q., Morrell, S.L., Duan, D.L., 2007. Delineation of *Chondrus* (Gigartinales, Florideophyceae) in China and the origin of *C. crispus* inferred from molecular data. Mar. Biol. Res. 3, 145–154.

Hu, Z.M., Guiry, M.D., Critchley, A.T., Duan, D.L., 2010. Phylogeographic patterns indicate transatlantic migration from Europe to North America in the red seaweed *Chondrus crispus* (Gigartinales, Rhodophyta). J. Phycol. 46, 889–900.

Hu, Z.M., Li, W., Li, J.J., Duan, D.L., 2011a. Post-Pleistocene demographic history of the North Atlantic endemic Irish moss *Chondrus crispus*: glacial survival, spatial expansion and gene flow. J. Evol. Biol. 24, 505–517.

Hu, Z.M., Uwai, S., Yu, S.H., Komatsu, T., Ajisaka, T., Duan, D.L., 2011b. Phylogeographic heterogeneity of the brown macroalga *Sargassum horneri* (Fucaceae) in the northwestern Pacific in relation to late Pleistocene glaciation and tectonic configurations. Mol. Ecol. 20, 3894–3909.

Hu, Z.M., Zeng, X.Q., Wang, A.H., Shi, C.J., Duan, D.L., 2004. An efficient method for DNA isolation from red algae. J. Appl. Phycol. 16, 161–166.

Hu, Z.M., Zhang, J., Lopez-Bautista, J., Duan, D.L., 2013. Asymmetric genetic exchange in the brown seaweed *Sargassum fusiforme* (Phaeophyceae) driven by oceanic currents. Mar. Biol. 160, 1407–1414.

Johnson, L.E., 1994. Enhanced settlement on microtopographical high points by the intertidal red alga *Halosaccion glandiforme*. Limnol. Oceanogr. 39, 1893–1902.

Johnson, L.E., Brawley, S.H., 1998. Dispersal and recruitment of a canopy-forming intertidal alga: the relative roles of propagule availability and post-settlement processes. Oecologia 117, 517–526.

Johnson, L.E., Brawley, S.H., Adey, W.H., 2012. Secondary spread of invasive species: historic patterns and underlying mechanisms of the continuing invasion of the European rockweed Fucus serratus in eastern North America. Biol. Invasions 14, 79–97.

Kamiya, M., Zuccarello, G.C., West, J.A., 2004. Phylogeography of *Caloglossa leprieurii* and related species (Delesseriaceae, Rhodophyta) based on the *rbc*L gene sequences. Jpn. J. Phycol. 52, 147–151.

Krueger-Hadfield, S.A., Collen, J., Daguin-Thiebaut, C., Valero, M., 2011. Genetic population structure and mating system in *Chondrus crispus* (Rhodophyta). J. Phycol. 47, 440–450.

Le Gall, L., Saunders, G.W., 2010. DNA barcoding is a powerful tool to uncover algal diversity: a case study of the Phyllophoraceae (Gigartinales, Rhodophyta) in the Canadian flora. J. Phycol. 46, 374–389.

Li, J.J., Hu, Z.M., Duan, D.L., 2015. Genetic data from the red alga *Palmaria palmata* reveal a mid-Pleistocene deep genetic split in the North Atlantic. J. Biogeogr. 42, 902–913.

Librado, P., Rozas, J., 2009. DnaSP v5: a software for comprehensive analysis of DNA polymorphism data. Bioinformatics 25, 1451–1452.

Lindstrom, S.C., 2008. Cryptic diversity and phylogenetic relationships within the *Mastocarpus papillatus* species comples (Rhodophyta, Phyllophoraceae). J. Phycol. 44, 1300–1308.

Lindstrom, S.C., Hanic, L.A., 2005. The phylogeny of North American *Urospora* (Ulotrichales, Chlorophyta) based on sequence analysis of nuclear ribosomal genes, introns and spacers. Phycologia 44, 194–201.

Lindstrom, S.C., Hughey, J.R., Martone, P.T., 2011. New, resurrected and redefined species of *Mastocarpus* (Phyllophoraceae, Rhodophyta) from the northeast Pacific. Phycologia 50, 661–683.

Lohrmann, N.L., Logan, B.A., Johnson, A.S., 2004. Seasonal acclimatization of antioxidants and photosynthesis in *Chondrus crispus* and *Mastocarpus stellatus*, two co-occurring red algae with differing stress tolerances. Biol. Bull. 207, 225–232.

Ludington, W.B., Callicott, K.A., Detomaso, A.W., 2004. Genetic variation in *Mastocarpus papillatus* (Rhodophyta) in central California using amplified fragment length polymorphisms. Plant Spec. Biol. 19, 107–113.

Maggs, C.A., Castilho, R., Foltz, D., Henzler, C., Jolly, M.T., Kelly, J., Olsen, J., Perez, K.E., Stam, W., Väinölä, R., Viard, F., Wares, J., 2008. Evaluating signatures of glacial refugia for North Atlantic benthic marine taxa. Ecology 89, S108–S122.

McNair, J.N., Newbold, J.D., Hart, D.D., 1997. Turbulent transport of suspended particles and dispersing benthic organisms: How long to hit bottom? J. Theor. Biol. 188, 29–52.

Neiva, J., Assis, J., Fernandes, F., Pearson, G.A., Serrão, E.A., 2014. Species distribution models and mitochondrial DNA phylogeography suggest an extensive biogeographical shift in the high-intertidal seaweed *Pelvetia canaliculata*. J. Biogeogr. 41, 1137–1148.

Neiva, J., Pearson, G.A., Valero, M., Serrão, E.A., 2012. Drifting fronds and drifting alleles: range dynamics, local dispersal and habitat isolation shape the population structure of the estuarine seaweed *Fucus ceranoides*. J. Biogeogr. 39, 1167–1178.

Nielsen, R., Wakeley, J., 2001. Distinguishing migration from isolation: a Markov chain Monte Carlo approach. Genetics 158, 885–896.

Olsen, J.L., Zechman, F.W., Hoarau, G., Coyer, J.A., Stam, W.T., Valero, M., Åberg, P., 2010. The phylogeographic architecture of the fucoid seaweed *Ascophyllum nodosum*: an intertidal 'marine tree' and survivor of more than one glacial-interglacial cycle. J. Biogeogr. 37, 842–856.

Pearse, D.E., Crandall, K.A., 2004. Beyond F_{ST}: analysis of population genetic data for conservation. Conserv. Genet. 5, 585–602.

Polanshek, A.R., West, J.A., 1977. Culture and hybridization studies on *Gigartina papillata* (Rhodophyta). J. Phycol. 13, 141–149.

Posada, D., Crandall, K.A., 1998. MODELTEST: testing the model of DNA substitution. Bioinformatics 14, 817–818.

Provan, J., Maggs, C.A., 2012. Unique genetic variation at a species' rear edge is under threat from global climate change. Proc. R. Soc. B 279, 39–47.

Provan, J., Wattier, R.A., Maggs, C.A., 2005. Phylogeographic analysis of the red seaweed *Palmaria palmata* reveals a Pleistocene marine glacial refugium in the English Channel. Mol. Ecol. 14, 793–803.

Ray, N., Currat, M., Excoffier, L., 2003. Intra-deme molecular diversity in spatially expanding populations. Mol. Biol. Evol. 20, 76–86.
Riginos, C., Henzler, C.M., 2008. Patterns of mtDNA diversity in North Atlantic populations of the mussel *Mytilus edulis*. Mar. Biol. 155, 399–412.
Robba, L., Russell, S.J., Barker, G.L., Brodie, J., 2006. Assessing the use of the mitochondrial *cox*1 marker for use in DNA barcoding of red algae (Rhodophyta). Am. J. Bot. 93, 1101–1108.
Rogers, A.R., Harpending, H., 1992. Population growth makes waves in the distribution of pairwise genetic differences. Mol. Biol. Evol. 9, 552–569.
Ronquist, F., Teslenko, M., van der Mark, P., Ayres, D.L., Darling, A., Höhna, S., Larget, B., Liu, L., Suchard, M.A., Huelsenbeck, J.P., 2012. MrBayes 3.2: efficient Bayesian phylogenetic inference and model choice across a large model space. Syst. Biol. 61, 539–542.
Siegenthaler, U., Stocker, T.F., Monnin, E., Luthi, D., Schwander, J., Stauffer, B., Raynaud, D., Barnola, J.M., Fischer, H., Masson-Delmotte, V., Jouzel, J., 2005. Stable carbon cycle-climate relationship during the late Pleistocene. Science 310, 1313–1317.
Tajima, F., 1989. Statistical method for testing the neutral mutation hypothesis by DNA polymorphism. Genetics 123, 585–595.
Teasdale, B.W., Klein, A.S., 2010. Genetic variation and biogeographical boundaries within the red alga *Porphyra umbilicalis* (Bangiales, Rhodophyta). Bot. Marina 53, 417–431.
Templeton, A.R., 1993. The 'Eve' hypothesis: a genetic critique and reanalysis. Am. Anthr. 95, 51–72.
Thompson, J.D., Gibson, T.J., Plewniak, F., Jeanmougin, F., Higgins, D.G., 1997. The CLUSTAL_X windows interface: flexible strategies for multiple sequence alignment aided by quality analysis tools. Nucl. Acids Res. 25, 4876–4882.
Wares, J.P., 2002. Community genetics in the Northwestern Atlantic intertidal. Mol. Ecol. 11, 1131–1144.
Wares, J.P., Cunningham, C.W., 2001. Phylogeography and historical ecology of the North Atlantic intertidal. Evolution 55, 2455–2469.
Zuccarello, G.C., Burger, G., West, J.A., King, R.J., 1999a. A mitochondrial marker for red algal intraspecific relationships. Mol. Ecol. 8, 1443–1447.
Zuccarello, G.C., Schidlo, N., McIvor, L., Guiry, M.D., 2005. A molecular re-examination of speciation in the intertidal red alga *Mastocarpus stellatus* (Gigartinales, Rhodophyta) in Europe. Eur. J. Phycol. 40, 337–344.
Zuccarello, G.C., West, J.A., 2002. Phylogeography of the *Bostrychia calliptera-B. pinnata complex* (Rhodomelaceae, Rhodophyta) and divergence rates based on nuclear, mitochondrial and plastid DNA markers. Phycologia 41, 49–60.
Zuccarello, G.C., West, J.A., Kamiya, M., King, R.J., 1999b. A rapid method to score plastid haplotypes in red seaweeds and its use in determining parental inheritance of plastids in the red alga Bostrychia (Ceramiales). Hydrobiologia 401, 207–214.
Zupan, J.R., West, J.A., 1988. Geographic variation in the life history of *Mastocarpus papillatus* (Rhodophyta). J. Phycol. 24, 223–229.